Universidad de Concepción
Departamento de Ingeniería Civil

Asociación Chilena de Sismología e Ingeniería Antisísmica

N° A10-17
CONSEQUENCES OF USING RAYLEIGH DAMPING IN INELASTIC RESPONSE HISTORY ANALYSIS

Finley A. Charney[1]

1.- Department of Civil and Environmental Engineering, Virginia Tech
200 Patton Hall, Blacksburg, Virginia, U.S.A.
e-mail: fcharney@vt.edu

ABSTRACT

This paper investigates the consequence of using Rayleigh proportional damping in the analysis of inelastic structural systems. The discussion is presented theoretically, as well as by example through the analysis of a simple 5-story structure. It is shown that when the stiffness portion of the system damping matrix is based on the original system stiffness, artificial damping is generated when the structure yields. When the damping matrix is based on the tangent stiffness but the Rayleigh proportionality constants are based on the initial stiffness, a significant but reduced amplification of damping occurs. When the damping is based on the tangent stiffness and on updated frequencies based on this stiffness, virtually no artificial damping occurs. The paper also investigates the influence on effective damping when localized yielding occurs in areas of concentrated inelasticity. In such cases it is possible to develop artificial viscous damping forces that are extremely high, but that are not easy to detect. Such artificial damping forces may lead to completely invalid analysis. The paper ends with recommendations for performing analysis where the artificial damping is eliminated, or at least controlled.

keywords: damping, inelastic behavior, modeling, response history analysis

1. INTRODUCTION

All building structures exhibit some degree of energy loss during free vibration. Traditionally, this energy loss is referred to *inherent damping*. The most significant source of inherent damping is internal friction in the structural materials, connections, and nonstructural components (Kareem and Gurley, 1996). Experiments have shown that inherent damping generally increases with displacement amplitude, and is not frequency dependent. Therefore, the most appropriate mathematical model for representing the damping is friction or hysteretic damping. Each of these approaches require nonlinear analysis, and this is

a serious complication when analyzing structures that are otherwise linear elastic. To overcome this difficulty, analysts usually linearize the inherent damping by assuming that it is viscous. Viscous damping is not amplitude dependent, but is frequency dependent.

The equations of motion for a linear elastic multiple degree of freedom system with linear viscous damping are as follows:

$$M\ddot{v}(t) + C\dot{v}(t) + Kv(t) = P(t) \tag{1}$$

where M is the mass matrix, C is the damping matrix, K is the elastic stiffness matrix, $P(t)$ is the dynamic load vector, and $v(t)$, $\dot{v}(t)$, and $\ddot{v}(t)$ are the displacements, velocities, and accelerations, respectively, at the various degrees of freedom. Two basic approaches are available for solving the dynamic equilibrium equations; direct integration and modal superposition. In both approaches, the mass and stiffness matrices are required. The development of these matrices is straightforward since they are based on easily identified and quantified physical properties. In the direct integration approach a damping matrix is also required, but the development of this matrix is not straightforward because there is no physical counterpart for the assumed viscous damping. While there is no requirement that the damping matrix used in direct integration be classical, Rayleigh damping, which is classical, is almost universally used.

In the modal superposition approach the full damping matrix is not required because damping values are directly assigned to the individual modes. The values in each mode may be specified arbitrarily, or through the use of a Caughey series (Caughey, 1960), of which Rayleigh damping is a special case. Given the modal damping ratios and the undamped modes shapes of the system, the damping matrix indicated in equation 1 may be recovered. There is generally no need to recover the damping matrix in ordinary analysis, although it may be useful to do so to understand how the form of this matrix affects the system response.

Given the system damping matrix, whether real or virtual, the response to any given load may be computed with great precision. The accuracy of the response, however, may be in question. The questionable accuracy arises from unforeseen consequences of the use of the viscous damping model. Fortunately, when using linear viscous damping to represent inherent damping in linear elastic systems, the variety of unforeseen consequences is limited, and the effect on computed response is usually insignificant. However, when the concept of linear viscous damping is applied to the analysis of structures with added damping, or to structures that behave inelastically, the variety and magnitude of unforeseen consequences can increase dramatically, and may lead to computed results that are invalid.

A complete explanation and quantification of the consequences of modeling damping in structures cannot be presented in a single technical paper. Hence, the scope of this paper is limited to the effects of the use of linear viscous damping in the response history analysis of inelastic systems. The discussion is further limited to the use of Rayleigh damping. Problems associated with the use of linear viscous damping in the analysis of linear elastic systems or systems which employ added damping devices are the subject of companion papers, in progress, but not yet submitted for publication.

The paper is also limited to the discussion of two specific problems associated with the use of Rayleigh damping in inelastic response history analysis. Each of these problems arise when there is a change in the tangent stiffness of the structure, and the effect is almost always manifested by unexpected increases in

effective damping. These increases in damping range from a few percent, to several hundred percent, and are extremely difficult to detect.

The first problem addressed is the effect of "global" changes in stiffness on the effective damping in the system. This problem was previously addressed in the paper by Leger and Dussault (1992). The second problem is related to "local" changes in stiffness which occur in plastic hinges and other areas of concentrated inelasticity. This problem, which is the more significant of the two, has been addressed by Bernal (1994).

This paper attempts to bring these discussions together, and to provide a holistic perspective of the problem. In most cases, the analysis and discussion is presented through use of the 5-story, 5-degree of freedom structure shown in Figure 1. The structure has a tridiagonal initial stiffness matrix and a diagonal mass matrix. These matrices are shown at the right of the figure. Note that the degrees of freedom are numbered from the top down. The viscous dashpots in Figure 1 represent a physical model of Rayleigh damping, as explained later in the paper. The initial (elastic) circular frequencies of the original undamaged structure are provided in column two of Table 1.

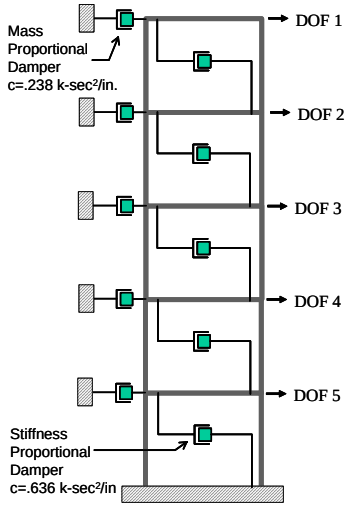

$$K = \begin{bmatrix} 497.7 & -497.7 & 0 & 0 & 0 \\ -497.7 & 993.5 & -497.7 & 0 & 0 \\ 0 & -497.7 & 993.5 & -497.7 & 0 \\ 0 & 0 & -497.7 & 993.5 & -497.7 \\ 0 & 0 & 0 & -497.7 & 993.5 \end{bmatrix} \text{ kips/in.}$$

$$M = \begin{bmatrix} 1.3 & 0 & 0 & 0 & 0 \\ 0 & 1.3 & 0 & 0 & 0 \\ 0 & 0 & 1.3 & 0 & 0 \\ 0 & 0 & 0 & 1.3 & 0 \\ 0 & 0 & 0 & 0 & 1.3 \end{bmatrix} \text{ kip-sec}^2\text{/in.}$$

$$C = \begin{bmatrix} 0.875 & -0.636 & 0 & 0 & 0 \\ -0.636 & 1.513 & -0.636 & 0 & 0 \\ 0 & -0.636 & 1.513 & -0.636 & 0 \\ 0 & 0 & -0.636 & 1.513 & -0.636 \\ 0 & 0 & 0 & -0.636 & 1.513 \end{bmatrix} \text{ kip-sec/in.}$$

FIGURE 1. EXAMPLE 5-STORY STRUCTURE

TABLE 1. MODAL PROPERTIES OF STRUCTURE ILLUSTRATED IN FIGURE 1

Mode	Circular Frequency, Rad/sec		
	(Original) No Damage	(Case 1) Uniform Damage	(Case 2) Varied Damage
1	5.6	3.4	2.4
2	16.2	11.5	9.8
3	25.6	18.1	16.4
4	32.9	23.3	23.2
5	37.5	26.5	31.0

2.0 RAYLEIGH DAMPING

In Rayleigh damping, it is assumed that the damping matrix is proportional to mass and stiffness, as follows

$$C = C_M + C_K = a_0 M + a_1 K \tag{2}$$

where the scalar coefficients a_0 and a_1 have units of 1/sec and sec, respectively.

A physical model for Rayleigh damping is shown in Figure 1. The dashpots between the floors represent the stiffness proportional damping, and the dashpots at the floor levels represent mass proportional damping. Note that the mass proportional dampers produce reactions external to the structure.

Using the mode shape matrix, Φ, and its transpose, equation 2 becomes

$$\Phi^T C \Phi = a_0 \Phi^T M \Phi + a_1 \Phi^T K \Phi \tag{3}$$

Due to the orthogonality property of the mode shapes (with respect to mass and stiffness), each of the matrix triple products in equation 3 is diagonal. Writing the equation for an individual mode j,

$$c_j = a_0 m_j + a_1 k_j \tag{4}$$

where the lower case terms represent the generalized mass, damping, and stiffness quantities. Dividing both sides of equation 4 by $2m_j\omega_j$, where ω_j is the undamped natural circular frequency in mode j , and noting that $\omega_j = \sqrt{k_j / m_j}$

$$\xi_j \equiv \frac{c_j}{2m_j\omega_j} = \frac{a_0}{2\omega_j} + \frac{a_1\omega_j}{2} \tag{5}$$

where ξ_j is the damping ratio in mode j.

The damping ratio in mode j cannot be determined without knowing the coefficients a_0 and a_1. These are determined by specifying damping ratios in any two modes, say k and n and writing equation 5 for each mode. These equations, solved simultaneously for a_0 and a_1 are represented in matrix form in equation 6. Once a_0 and a_1 are determined, the damping ratio in any other mode(s) may be determined from equation 5.

$$\begin{Bmatrix} \xi_k \\ \xi_n \end{Bmatrix} = \frac{1}{2}\begin{bmatrix} 1/\omega_k & \omega_k \\ 1/\omega_n & \omega_n \end{bmatrix}\begin{Bmatrix} a_0 \\ a_1 \end{Bmatrix} \tag{6}$$

It is noted that there is no requirement that the frequencies in equation 6 represent actual frequencies in the structural system. Any two damping values at any two frequencies will define a damping curve. In practice, however, the specified frequencies and damping values are almost always selected to correspond to actual system frequencies.

The usual approach with Rayleigh damping is to specify the a_0 and a_1 values for the entire system, in which case the damping matrix is formed internally by the program. It is also possible (in some cases) to

invoke the damping through the use of discrete dashpots, as shown in Figure 1. The author prefers this method because the forces in the damping system may be easily monitored. Finally, it is noted that some programs, such as Drain-2DX (Prakash, et al., 1993), allow the specification of mass and stiffness proportional damping terms for only those masses and elements that are selected by the user.

As mentioned earlier in this paper, Rayleigh damping is a special case of Caughey damping, where the damping matrix is given by the following series:

$$C = M \sum_{b} a_b [M^{-1} K]^b \qquad (7)$$

where the index b may theoretically take any integer values. Rayleigh damping is generated by a two-term series with b equal to zero and one. As discussed later in this paper, Bernal (1994) suggest the use of equation 7 with b less than or equal to zero.

2.1 Rayleigh Damping for Elastic System as Depicted in Figure 1

Rayleigh damping was computed for the structure in Figure 1 by setting a damping ratio of 0.02 in modes 1 and 3, resulting in a_0=0.183 and a_1=0.00128. Using these coefficients, the system damping matrix is as shown at the lower right of Figure 1. As expected, this matrix has the same profile as the stiffness matrix. A physical representation of the damping matrix is shown at the left of Figure 1. The mass proportional dashpots have a damping constant C_M of 0.183(1.30)=0.238 k-sec/in., and the stiffness proportional dashpots have a damping constant C_K=497(0.00128)=0.636 k-sec/in.

A plot of the damping relationship of equation 5, using a_0=0.183 and a_1=0.00128 is shown in Figure 2. In the figure, the mass and the stiffness proportional parts of the damping relationship are shown separately, where it may be seen that the mass proportional component decreases with increased frequency, and the stiffness proportional term increases with increased frequency.

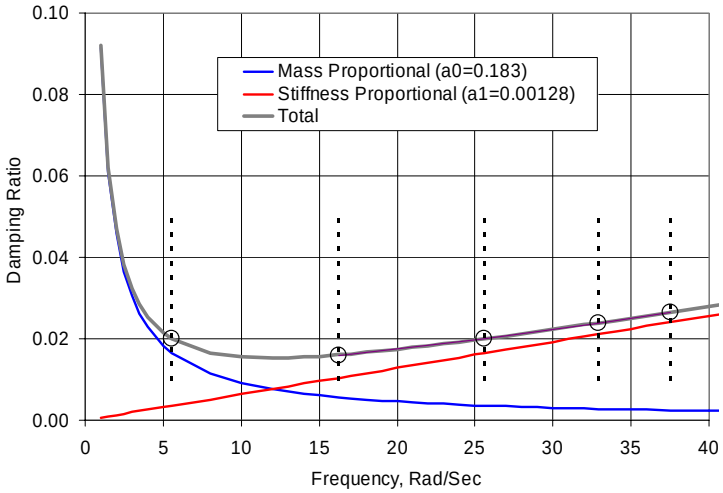

FIGURE 2. RAYLEIGH PROPORTIONAL DAMPING CURVES

Figure 2 also shows, with vertical dashed lines, the natural frequencies of the structure, and the damping ratios that occur at these frequencies. It is clear from equation 5 and Figure 2 that it is impossible to obtain a negative damping ratio at any frequency. However, it appears that frequency shifts to the left

may result in higher than expected damping in the lower modes. Frequency shifts, if they occur, would be due to changes in the stiffness matrix due to yielding. This phenomena is examined next with respect to the structure of Figure 1.

3. USING RAYLEIGH DAMPING IN INELASTIC RESPONSE

When the system responds inelastically, the stiffness term indicated in equation 1 changes. These changes can be abrupt or gradual, depending on the mathematical model being used. The changes are also nonuniform through the structure. When Rayleigh proportional damping is used, the analyst has three basic approaches to deal with the inelastic response. These approaches, described below, are labeled **A**, **B**, **C** for future reference.

Approach A) The damping matrix is computed on the basis of the initial stiffness and this damping matrix is used throughout the response. Hence, the damping matrix developed in equation 2 (repeated below as equation 8) is used for each step in the analysis.

$$C_A(t) = a_0 M + a_1 K \tag{8}$$

This damping matrix is constant throughout the analysis. At any step in the analysis in which the tangent stiffness is not equal (or proportional) to the elastic stiffness, the damping matrix will be nonclassical because the *current* mode shapes will not diagonalize *K*.

Approach B) The a_0 and a_1 proportionality terms are computed on the basis of the initial stiffness, and the damping matrix is updated each time the tangent stiffness changes. The damping matrix is

$$C_B(t) = a_0 M + a_1 K_t \tag{9}$$

where the subscript *t* on the *K* term represent the tangent stiffness. In this case, the damping matrix will be classical at each step in the analysis because the current mode shapes will diagonalize K_t.

Approach C) The a_0 and a_1 terms are recomputed each time the stiffness changes, and the damping matrix is reformed on this basis (assuming that the damping ratios in the specified modes do not change, regardless of modal frequency). In this case, the damping matrix is given by

$$C_C(t) = a_{0t} M + a_{1t} K_t \tag{10}$$

where the added subscript *t* on the a_0 and a_1 terms in equation 10 indicate that these are based on the tangent stiffness. As with approach **B**, the damping matrix will be classical.

It is noted that a principal disadvantage of approach **C** is that the two modal frequencies ω_k and ω_m on which a_{0t} and a_{1t} are based (see equation 6) must be recomputed with each change in stiffness.

In the following discussion the implication of the use of Rayleigh proportional damping in the analysis of inelastic systems are examined from the perspective of the entire structure (global stiffness changes) and from the perspective of local stiffness changes.

3.1 The Effect of Global Stiffness Changes on Structures Modeled with Rayleigh Damping

Given any damping matrix, classical or nonclassical, the damping values in each mode may be found by the modal strain energy approach, shown in equation 11, which is effectively a rearrangement of equation 3. For classically damped systems the resulting damping ratios are exact, and for nonclassical systems they are approximate.

$$\xi_j = \frac{\phi_j^T C \phi}{2\omega_j \phi_j^T M \phi_j} \tag{11}$$

The effects of the different methods of establishing damping in inelastic systems are examined with respect to the structure of Figure 1. Two different cases are investigated. In the first case the entire stiffness matrix is assumed to reduce to 50% of its original value. The mode shapes for this system are identical to those of the original system, and the frequencies for each mode are $\sqrt{0.5} = 0.707$ times the original frequencies. The frequencies for this uniformly damaged system are shown in column three of Table 1.

In the second case the stiffness properties change nonuniformly along the height. The stiffness of the individual levels of the structure, from top down, are 0.9, 0.7, 0.5, 0.3, and 0.1 times the original stiffness, respectively. These ratios represent significant yielding at the base of the structure and little yielding at the top. There is no simple relationship between the modal properties of the original system and the system with nonuniform stiffness changes. The frequencies for this system are shown in the last column of Table 1.

The results for the structure with the uniform stiffness change are shown in Figure 3, which is a plot of the damping vs frequency curves for the four different approaches **O**, **A**, **B**, and **C**. In each case the damping ratios were computed using equation 11. Approach **O** represents the original elastic system without the stiffness changes. Note that the graph has two sets of vertical dashed lines. The vertical lines that extend to the bottom of the plot represent the original frequencies, and the vertical lines that extend to the top of the plot represent the frequencies for the damaged system.

As observed from Figure 3, the effective damping values for approach **A**, based on the original damping matrix and the revised frequencies are somewhat larger than the original values. In fact, the damping value at each revised frequency is exactly 1.414 times the original damping value at the corresponding original frequency. Mathematically, the damping curve for approach **A** is $\xi(\omega) = 0.5(0.183/\omega + 0.00257\omega)$. The mass proportional coefficient is the same as that for the original system, and the stiffness proportional coefficient is two times that of the original system. Hence, the damping versus frequency curve for the revised system is *different* from that of the original system.

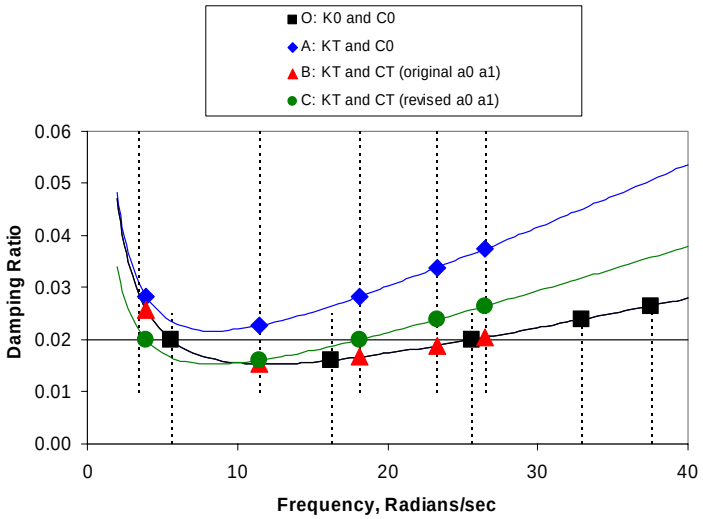

FIGURE 3. DAMPING VS FREQUENCY FOR STRUCTURE WITH UNIFORM STIFFNESS CHANGE

The damping values for approach **B,** which is based on the revised system with the damping matrix based on the tangent stiffness and the original a_0 and a_1 values, lie on the same curve as those for the original system. However, the damping values at each of the revised frequencies are different than in the original system because the frequencies have shifted to the left in the figure.

The damping values for approach **C**, lie on a different curve, with the equation for the curve being $\xi(\omega) = 0.5(0.129/\omega + 0.00181\omega)$. Here, the mass coefficient is 0.707 times the mass coefficient for the original curve, and the stiffness coefficient is 1.414 times that for the original curve. The damping values at the five revised frequencies are *exactly the same* as the damping values from case **O** using the original frequencies.

In Figure 4, the damping ratios in each mode for approaches **A**, **B**, and **C**, divided by the original damping ratio (approach **O**), are plotted against mode number. As may be seen, approach **A** gives a consistent ratio of 1.414, approach **B** has a varying ratio, and approach **C** has a ratio of exactly 1.0 for each mode.

The results for the structure with the nonuniform stiffness change (Case 2) are presented in Figures 5 and 6. These figures plot damping ratio vs frequency, and the ratio of damping ratios vs mode number, respectively.

As seen in Figure 5, the damping ratios for approach **A**, indicated by the solid diamonds, do not fall on any well-defined curve. This is due to the fact that the damping matrix for this approach, formed as a linear combination of mass and *initial* stiffness, is nonclassical[1] when the stiffness changes. As may be seen from Figure 6, there is a considerable increase in the damping ratios for approach **A.** For the lower

[1] For systems with very high nonclassical damping the damping ratios should theoretically be computed using a complex arithmetic based state-space approach instead of the modal strain energy approach. For the case discussed herein, where the damping ratios are very low, there is virtually no difference between the damping ratios computed using these two approaches.

modes, the damping ratio has increased by a factor of 2.5, which may have a very significant effect on the computed results.

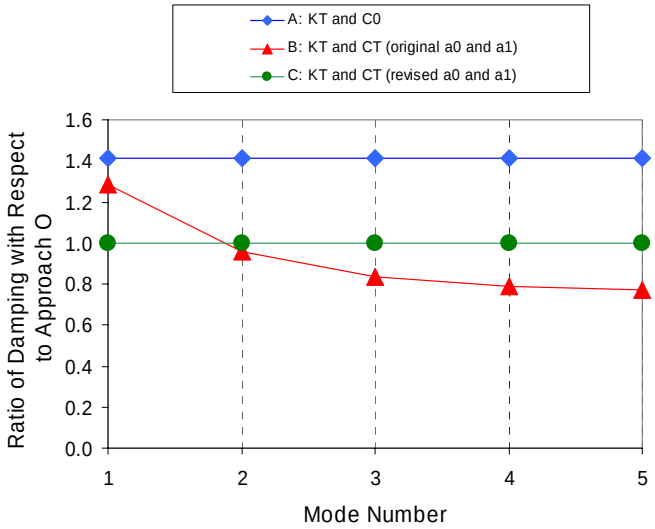

FIGURE 4. RATIO OF DAMPING RATIOS VS MODE NUMBER FOR STRUCTURE WITH UNIFORM STIFFNESS CHANGE

For approach **B**, where the damping matrix is based on the tangent stiffness and on the original a_0 and a_1 values (and is therefore classical), the damping values fall on the curve $\xi(\omega) = 0.5(0.183/\omega + 0.00128\omega)$. This curve is identical to the curve for the elastic system, but the damping values have changed because the frequencies have changed. As indicated in Figure 6, the damping in the first mode has effectively doubled, but the ratios for the other modes are close to the original values.

For approach **C**, the damping curve in Figure 5 is given by $\xi(\omega) = 0.5(0.0.084/\omega + 0.00213\omega)$, and the damping values at all frequencies are very close to those for the original system.

As shown for the results of the uniform and nonuniform damage cases presented above, the actual damping obtained at each time step of a response history analysis depends on the method for computing damping (approaches **A**, **B**, or **C**), and on the damage state in the structure at that point in time. It is clear that the largest increases in effective damping occur in approach **A**, where the damping matrix is based on the original system state.

Approach **B**, which bases the damping matrix on the current tangent stiffness, but using the original proportionality coefficients a_0 and a_1, produces modal damping values that are different than the elastic system, but on the same Rayleigh damping curve as the original system. Hence, and frequency shift to the left will generally result in higher damping in the mass proportional dominated lower modes, and lower damping in the stiffness proportional dominated higher modes.

Approach **C** always produces damping values that are close to that of the original system. However, this approach may be impractical due to the necessity to recompute the modal frequencies at each step. It is noted that Leger and Dussalt (1992) recommend this approach, with the further stipulation that the two

frequencies at which the Rayleigh damping is set be the first mode, and the lowest mode for which the cumulative effective mass is 90% of the total mass.

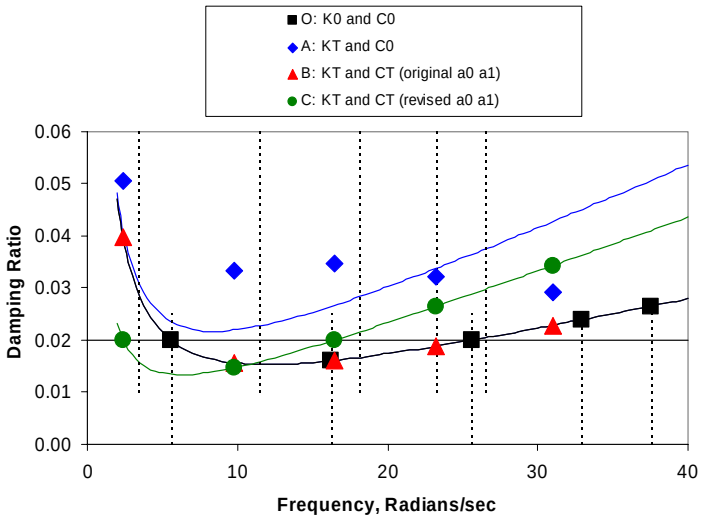

FIGURE 5. DAMPING VS FREQUENCY FOR STRUCTURE WITH NONUNIFORM STIFFNESS CHANGE

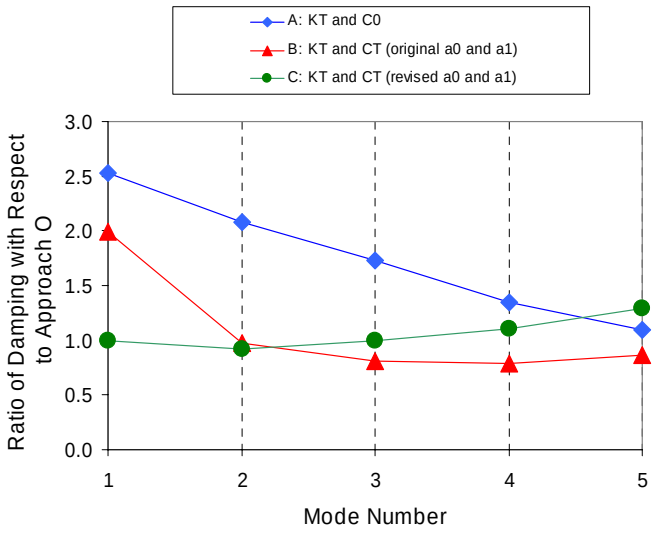

FIGURE 6. RATIO OF DAMPING RATIOS VS MODE NUMBER FOR STRUCTURE WITH UNIFORM STIFFNESS CHANGE

A potential problem with approaches **B** and **C** is that the stiffness component of effective damping may be negative if the tangent stiffness for the structure at any step in the analysis is negative. This can occur, for example, when the structure has significant damage and second order (P-Delta) effects are included in the analysis. One way to avoid this problem is to not include the geometric stiffness in that part of the tangent stiffness on which the damping is based.

In the previous discussion, it might be inferred that the increases in damping that may occur in association with approaches **A** and **B** are not desirable, and should be avoided. This is not necessarily the case. Consider, for example, a reinforced concrete structure. Prior to an earthquake, the damping properties of the structure are uniform throughout, and may be thought of as a material property (e.g. loss modulus). During the earthquake the individual members (beams, columns, walls) of the structure are damaged nonuniformly; there is very significant damage in the hinging regions and there is minor but not insignificant damage in the remainder of the member. Most analysis programs ignore the fact that the damage in the remainder of the member contributes to the energy dissipation, and therefore to the damping in the system. Approaches **A** and **B** may be tailored to include this behavior.

3.2 The Effect of Local Stiffness Changes on Structures Modeled with Rayleigh Damping

For any system the global stiffness changes are an accumulation of the changes in the individual elements. For the idealized structure of Figure 1, the global changes were represented by arbitrary changes in the system stiffness matrix. The effect of local stiffness changes are now investigated, and to facilitate this investigation, each story of the structure of Figure 1 has been modeled as shown in Figure 7. In this one-story structure the lateral flexibility has two contributions; flexural deformations of the beams and columns, and concentrated rotational deformations in "plastic hinges" at the beam-column intersection. The properties of the beams, columns, and rotational springs were set to produce a story stiffness exactly equal to that for the structure shown in Figure 1.

As modeled, each of the one-story bents has five degrees of freedom; one lateral displacement and four rotations, two at each beam-column joint. The plastic hinge rotation is equal to the difference in the rotations at each joint. The only mass that is active at each level is the mass associated with the lateral degree of freedom, and this mass is the same as the story mass of the structure depicted in Figure 1. There are no rotational masses.

When five of the one-story frames of Figure 7 are stacked on top of each other, the resulting structure has 25 degrees of freedom. When the massless rotational degrees of freedom are condensed out, the resulting structure has exactly the same stiffness matrix as the structure of Figure 1. The frequencies for the system are tabulated in the second column of Table 1. Rayleigh proportional damping as based on the initial stiffness is set to produce 2% damping in the first and third modes. Hence, the damping curve for the structure is identical to that shown in Figure 2. The equation for this curve is $\xi(\omega) = 0.5(0.183/\omega + 0.00128\omega)$.

A response history analysis is performed for the structure using the El-Centro ground motion scaled to produce a peak ground acceleration of 0.62g. Three different sets of properties were used, with the principal difference being the relative stiffness contributed by the beams and columns and rotational springs. These properties are listed in Table 2. For the first case, the beams and columns are effectively rigid, and the rotational spring is relatively flexible. In the last case, the spring is very rigid, and the beams and columns are relatively flexible. Case 2 represents an intermediate distribution of stiffness. The rotational springs are assumed to yield at a moment of 11250 in-k, and there is no strain hardening after yield. Under this condition, each one-story frame has an identical lateral pushover curve.

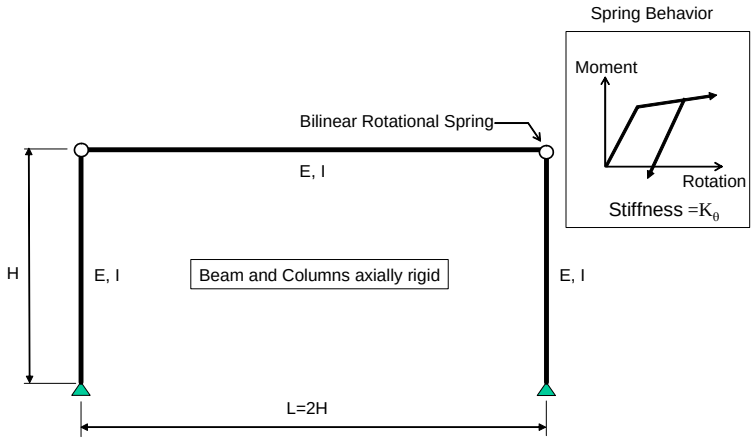

FIGURE 7. DETAILED STORY MODEL FOR 5-STORY STRUCTURE

TABLE 2. ANALYSIS PROPERTIES FOR INELASTIC RESPONSE HISTORY ANALYSIS

Model Case	Moment of Inertia of Beam and Column (in^4)	Rotational Stiffness of Bilinear Hinge (in-k/radian)
1	100000000	5.60×10^6
2	40000	1.046×10^7
3	19000	2.885×10^8

When an elastic analysis is performed for these systems the computed response histories are identical. If the damping in the system is associated with only the five lateral degrees of freedom[2], the inelastic responses are also identical. When the damping matrix is based on the full 25 degree of freedom system the response histories are quite different. These differences are evident in the response histories shown in Figure 8. Only the first ten seconds of the computed response is shown.

The roof displacement histories are shown in Figure 8(a). The thin line in the figure is for the system with relatively flexible hinge springs, and the thick line is for the system with stiff springs. The displacements, although different, are not tremendously different, and the analyst would have no reason to suspect the response given by the system modeled with stiff hinges. The rotational velocity in the hinges at the lower level of the structure is given in Figure 8(b). The differences here are more significant that in Figure 8(a). Note, however, that a typical analyst would not plot these rotational velocities, and he or she would still not be suspicious of the results.

In Figure 8(c), the viscous moments histories in the lower level hinges are plotted. Few programs that provide Rayleigh proportional damping have the capability to plot these curves, so the analyst may not even be aware that the moments exist[3]. These moments are, however, extremely important. For Model 1,

[2] In this case the 5 by 5 damping matrix is expanded to a 25 by 25 matrix by filling massless rows and columns with zeros.
[3] It is noted that the author of this paper first became aware of the presence of these fictitious moments when he *accidentally* plotted them in a special post-processor he developed for use with Drain-2D. It is the discovery of these moments that motivated this paper.

which uses the more flexible hinge spring, the viscous moments are negligible. For Model 2, and most particularly for Model 3, these moments are quite large, and exceed the moment capacity (11250 in-k) of the hinge. These moments are completely fictitious, and do not exist in the actual structure. They are a remnant of initial stiffness based Rayleigh proportional damping.

The artificial viscous moments in the hinges are transferred to the beams and columns. The viscous moments that are transferred into the columns appear in the output as elastic moments, and are added to the moment that results from the product of nodal displacements and the element stiffness. These combined moments produce shears, the total of which for the lowest story is plotted in Figure 8(d). These shears are the base shears. As may be observed, the shears for Model 3 are more than twice the shears from Model 1, which are the correct values.

The viscous moments that occur in the hinges are simply the product of the rotational deformational velocity, $\dot{\theta}$, the spring rotational stiffness K_θ, and the stiffness proportional damping constant a_1. When a spring with a reasonable stiffness is used, this product is insignificant because the stiffness proportional damping constant is quite low (0.00183 in the present case), as is the typical rotational velocity (less than 1 radian/second in the current example). The problem occurs when artificially high stiffness is used to model the hinges. A similar problem may occur for friction dampers and gap elements.

The problem described above occurs only when the damping is based on the initial stiffness. When this is the only option in the program being used, the stiffness proportional damping constant a_1 should be set to zero for artificially stiff elements. Drain 2Dx provides this option, as do several other popular programs. If this can not be done, the analyst should attempt to reduce the stiffness of the offending element.

Bernal (1994) analyzes a similar phenomenon in his paper. He notes that the problem is associated with the fact that the nodes to which the springs are connected have no rotational mass, and suggests that a possible solution is to use Caughey damping with *b* values less than or equal to zero (see equation 7). One example would be to base the damping on $b = -1$ and $b = 0$. According to equation 7, this results in a damping matrix of the form $C = a_{-1}MK^{-1}M + a_0M$. Bernal's suggestion has the effect of not assigning any stiffness proportional damping to massless degrees of freedom. Note, however, that the problem will persist if some non-zero mass is assigned to the rotational degrees of freedom in the example problem. Another disadvantage to this approach is the use of the inverse of *K* in the first term. The inverse is not particularly easy to compute, and it does not have the same storage profile as *K*. This complicates solution efficiency. If the principal goal is to eliminate those damping terms associated with massless DOF, a much simpler approach is use $C = \alpha M + \beta JKJ$ where *J* is a diagonal matrix with ones at each dynamic DOF (with mass) and zeros at all massless DOF. The proportionality constants α and β would be determined by trial and error, with the modal strain energy approach being used to find the damping in each mode. It is noted that the damping matrix so-formed is nonclassical.

A better solution is to use a tangent stiffness based damping, such as approach **B** or **C** described earlier. The best strategy, of course, is to eliminate the use of viscous damping altogether, and use frictional or hysteretic devices to represent inherent damping. This does not add significant difficulty in the analysis, because a nonlinear approach is already necessary to accommodate the large-scale inelastic behavior. Additionally, frictional and hysteretic damping is much more in tune with the actual behavior of the structure than is viscous damping, which is entirely fictitious.

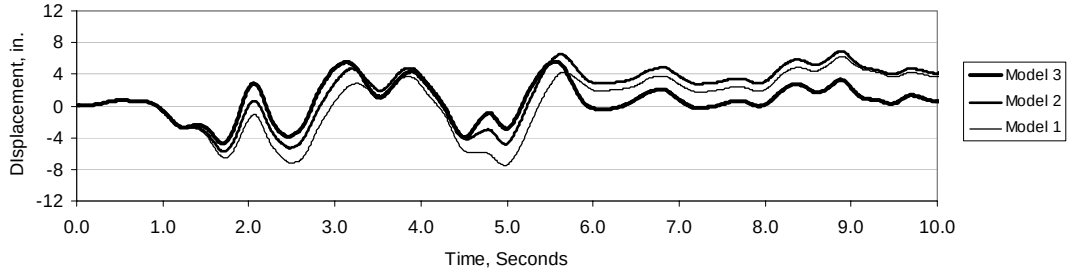

(a) Roof Displacement

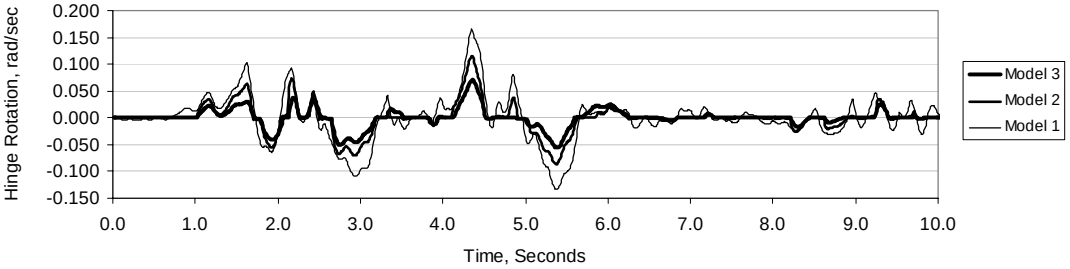

(b) Hinge Rotational Velocity

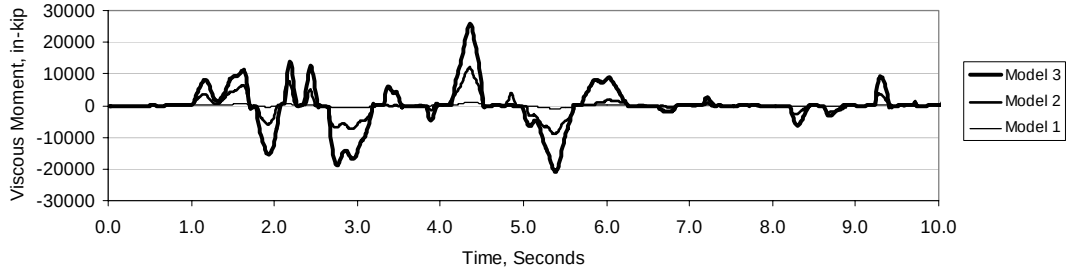

(c) Hinge Viscous Moment

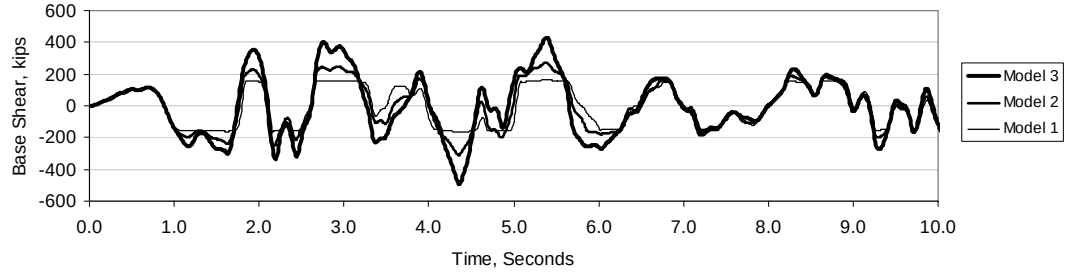

(d) Base Shear

FIGURE 8. RESULTS OF RESPONSE HISTORY ANALYSIS

4. SUMMARY AND CONCLUSIONS

In this paper the consequence of using Rayleigh proportional damping in the analysis of inelastic systems is discussed through theoretical development, and through example analysis of a simple 5-story structure. In the theoretical development, it is mentioned that the original motivation for the development of Rayleigh Proportional damping was to provide a damping matrix that is diagonalized by the undamped mode shapes. When inelastic structures are analyzed, this benefit of proportional damping disappears. Nevertheless, the vast majority of commercial and research software continues to use Rayleigh damping.

When it is assumed that the damping matrix is proportional to mass and initial stiffness, artificial damping may be generated in the lower modes, with the effective damping increasing several hundred percent. When the damping matrix is proportional to tangent stiffness but the proportionality coefficients are based on elastic stiffness, a moderate degree of artificial damping may be generated. When the damping matrix is based on tangent stiffness and the proportionality constants are also based on tangent stiffness, there is no artificial damping. Although significant artificial damping may be generated by use of Rayleigh damping, it cannot be said that the benefits are always detrimental. For example, such increases in damping may be desired in the analysis of reinforced concrete structures where the additional damping represents damage in regions of the structure for which hysteretic energy dissipation is not provided.

In some cases the use of initial stiffness proportional damping may produce extreme errors. This occurs when rigid elements, used to model gap openings or plastic hinges, have a change in state. Following the change of state, large viscous damping forces may be generated. These forces are the product of the post-event deformational velocities multiplied by the initial stiffness and by the stiffness proportional damping term. Such forces are artificial, and may be orders of magnitude greater than the actual strength of the element that resists the same deformations. When the damping is based on initial stiffness, the best approach to avoid these artificial forces is to provide a stiffness proportional damping multiplier of zero for these elements. An alternate approach is to develop an "auxiliary" damping structure that is adjacent to the main structure. The use of tangent stiffness proportional damping, when available, will also avoid the problem. An even better solution would be to eliminate the use of viscous damping altogether, and utilize nonlinear frictional or hysteretic damping.

5. REFERENCES

Bernal, D., (1994). "Viscous Damping in Inelastic Structural Response", *Journal of Structural Engineering*, ASCE, Vol. 120, No.4, 1240-1254.

Caughy, T.K., (1960). Classical Normal Modes in Damped Linear Systems", Journal of Applied Mechanics, 27, 269-271.

Kareem, A, and Gurley, K., (1996). "Damping in structures: its valuation and treatment of uncertainty", *Journal of Wind Engineering and Industrial Aerodynamics*, 59, 131-157.

Leger, P., and Dussault, S., (1992). "Seismic-Energy Dissipation in MDOF Structures", *Journal of Structural Engineering*, ASCE, Vol. 118, No.5, 1251-1269.

Prakash, C., Powell, G., and Campbell, S., (1993). *Drain-2DX Program Description and User Guide*, Department of Civil Engineering, University of California, Berkeley.